Excited Singlet States of "Hairpin" Polyenes[1a]

Wolfgang Frölich,[1b] Harry J. Dewey,[1c] Hans Deger,[1b] Bernhard Dick,[1b] Kenneth A. Klingensmith,[1c] Wilhelm Püttmann,[1b] Emanuel Vogel,*[1b] Georg Hohlneicher,*[1b] and Josef Michl*[1c]

Contribution from the Institute for Organic Chemistry, University of Cologne, Cologne, Germany, and the Department of Chemistry, University of Utah, Salt Lake City, Utah 84112.
Received December 29, 1982

Abstract: The synthesis and the UV–visible absorption, polarized fluorescence, and MCD spectra of six U-shaped "hairpin" polyenes (**1–6**) are reported. Qualitative arguments and results of π-electron calculations permit the identification of four excited singlet states and their assignment to mixtures of singly and doubly excited configurations. The hairpin polyenes represent a link between the all-trans polyenes on the one hand and the annulenes and acenes on the other hand: they possess the topology of the former and a geometry near that of the latter. The understanding of their electronic states offers a unified view of low-energy transitions in polyenes and aromatics, which accounts for their differences in a simple and intuitive manner.

Introduction

The electronic excited states of conjugated polyenes have attracted the attention of spectroscopists and theoreticians for a long time, at least partly because of their relation to the process of vision. For many years, the spectroscopy of the optically allowed transition from the A ground state to excited B states, easily described in the MO framework with one-electron excitations,[2,3] commanded nearly exclusive attention. This was true in spite of the fact that MO calculations with no configuration interaction and those which consider only singly excited configurations predicted a low-energy excited state of A symmetry not much higher than the first B state. It is understandable considering that electric dipole transitions of the A_g–A_g type are symmetry-forbidden in all-trans polyenes.[4]

In retrospect, the first calculation which was able to handle both the A_g and the B_u types of states properly appeared[5] in 1954. It was followed by several extensive fundamental studies[6–9] in the 1960's. Three of these calculations[6–8] were based on the MO–CI method with inclusion of multiply excited configurations, one on the VB method with the inclusion of ionic structures.[9] They concluded that the lowest among the A_g states is of covalent (in VB language) and partly "doubly excited" (in MO language) character and that its energy should be below that or about equal to that of the lowest among the B_u states, since the former is preferentially stabilized by configuration mixing. At the time, there was no convincing experimental support for this conclusion, and it represented a true theoretical prediction.

In these remarkable early papers, the importance of the A_g state for polyene photochemistry was discussed in detail,[9] the detectability of these states in two-photon absorption was predicted,[7] the role of the steepness of the assumed two-center electron repulsion parameter function in semiempirical calculations was analyzed,[7] and it was noted that the effects of the inclusion of multiply excited configurations in the CI procedure should become smaller as the molecule becomes more compact.[7]

In the 1970's, polyene spectroscopy has witnessed a renaissance, triggered by the experimental observation of the A_g state in diphenyloctatetraene.[10] By now, this state has been directly observed in several simple polyenes, using both one-photon[11] and two-photon[12] absorption experiments. Considerable advances have also been made in ab initio[13] and in semiempirical[14–17] calculations

(1) (a) Dedicated to Professor Albert Weller on the occasion of his 60th birthday. (b) University of Cologne. (c) University of Utah.

(2) (a) Mulliken, J. S. *J. Chem. Phys.* **1939**, *7*, 121, 339; (b) Mulliken, R. S. *Ibid.* **1939**, *7*, 364.

(3) Pariser, R.; Parr, R. G. *J. Chem. Phys.* **1953**, *21*, 767. See also Parr, R. G.; Mulliken, R. S. *Ibid.* **1950**, *18*, 1338.

(4) For a time, it was believed[3,5] that the calculated excited A_g state of butadiene should be identified with a spectral feature at 50000 cm^{-1} as proposed in ref 2b.

(5) Pullman, A.; Baudet, J. *C. R. Acad. Sci.* **1954**, *238*, 241.

(6) Allinger, N. L.; Tai, J. C. *J. Am. Chem. Soc.* **1965**, *87*, 2081.

(7) Koutecký, J. *J. Chem. Phys.* **1967**, *47*, 1501.

(8) Buenker, R. J.; Whitten, J. C. *J. Chem. Phys.* **1968**, *49*, 5381.

(9) Van der Lugt, W. Th. A. M.; Oosterhoff, L. J. *J. Am. Chem. Soc.* **1969**, *91*, 6042.

(10) Hudson, B. S.; Kohler, B. E. *Chem. Phys. Lett.* **1972**, *14*, 2991; *J. Chem. Phys.* **1973**, *59*, 4984; at that time, the observation of an excited state with an even higher contribution from doubly excited configurations was also reported for a more complicated π-electron system: Downing, J.; Dvořák, V.; Kolc, J.; Manzara, A.; Michl, J. *Chem. Phys. Lett.* **1972**, *17*, 70; Kolc, J.; Downing, J. W.; Manzara, A. P.; Michl, J. *J. Am. Chem. Soc.* **1976**, *98*, 930.

(11) (a) Hudson, B. S.; Kohler, B. E. *Ann. Rev. Phys. Chem.* **1974**, *25*, 437, and references cited therein. (b) Christensen, R. L.; Kohler, B. E. *Photochem. Photobiol.* **1973**, *18*, 293. (c) Gavin, R. M., Jr.; Risemberg, S.; Rice, S. A. *J. Chem. Phys.* **1973**, *58*, 3160. (d) Gavin, R. M., Jr.; Rice, S. A. *Ibid.* **1974**, *60*, 3231. (e) Karplus, M.; Gavin, R. M., Jr.; Rice, S. A. *Ibid.* **1975**, *63*, 5507. (f) McDiarmid, R. *Chem. Phys. Lett.* **1975**, *34*, 130. (g) Christensen, R. L.; Kohler, B. E. *J. Chem. Phys.* **1975**, *63*, 1837; *J. Phys. Chem.* **1976**, *80*, 2197. (h) Thrash, R. J.; Fang, H. L. B.; Leroi, G. E. *J. Chem. Phys.* **1977**, *67*, 5930. (i) Andrews, J. R.; Hudson, B. S. *Chem. Phys. Lett.* **1978**, *57*, 600. **1979**, *60*, 380. (j) Gavin, R. M., Jr.; Weisman, C.; McVey, J. K.; Rice, S. A. *J. Chem. Phys.* **1978**, *68*, 522. (k) Andrews, J. R.; Hudson, B. S. *J. Chem. Phys.* **1978**, *68*, 4587. (l) Becker, R. S.; Das, P. K.; Kogan, G. *Chem. Phys. Lett.* **1979**, 463. (m) Doering, J. P. *J. Chem. Phys.* **1979**, *70*, 3902. (n) Granville, M. F.; Holtom, G. R.; Kohler, B. E. *Ibid.* **1980**, *72*, 4671. (o) Doering, J. P.; McDiarmid, R. *Ibid.* **1980**, *73*, 3617. (p) McDiarmid, R.; Doering, J. P. *Ibid.* **1980**, *73*, 4192. (q) Lasaga, A. C.; Aerni, R. J.; Karplus, M. *Ibid.* **1980**, *73*, 5230. (r) D'Amico, K. L.; Manos, Ch.; Christensen, R. L. *J. Am. Chem. Soc.* **1980**, *102*, 1777. (s) Vaida, V.; McClelland, G. M. *Chem. Phys. Lett.* **1980**, *71*, 436. (t) Granville, M. F.; Kohler, B. E.; Snow, J. B. *J. Chem. Phys.* **1981**, *75*, 3765. (u) Heimbrock, L. A.; Kenny, J. E.; Kohler, B. E.; Scott, G. W. *Ibid.* **1981**, *75*, 4338. (v) Horowitz, J. S.; Goldbeck, R. A.; Kliger, D. S. *Chem. Phys. Lett.* **1981**, *80*, 229. (w) Chaltopadhyay, S. K.; Das, P. K. *Ibid.* **1982**, *87*, 145.

(12) (a) Johnson, P. M. *J. Chem. Phys.* **1976**, *64*, 4638. (b) Holtom, G. R.; McClain, W. M. *Chem. Phys. Lett.* **1976**, *44*, 436. (c) Parker, D. H.; Sheng, S. J.; El-Sayed, M. A. *J. Chem. Phys.* **1976**, *65*, 5534. (d) Fang, M. L. B.; Thrash, R. S.; Leroi, G. E. *Ibid.* **1977**, *67*, 3389. (e) Twarowski, A. J.; Kliger, D. S. *Chem. Phys. Lett.* **1977**, *50*, 36. (f) Vaida, V.; Turner, R. E.; Casey, J. L.; Colson, S. D. *Ibid.* **1978**, *54*, 25. (g) Birge, R. R.; Bennett, A.; Pierce, B. M.; Thomas, T. M. *J. Am. Chem. Soc.* **1978**, *100*, 1533. (h) Parker, D. H.; Berg, J. O.; El-Sayed, M. A. *Chem. Phys. Lett.* **1978**, *56*, 197. (i) Granville, M. F.; Holtom, G. R.; Kohler, B. E.; Christensen, R. L.; D'Amico, K. L. *J. Chem. Phys.* **1979**, *20*, 593. (j) Rothberg, L. J.; Gerrity, D. P.; Vaida, V. *Ibid.* **1980**, *73*, 5508.

(13) (a) Shih, S.; Buenker, R. J.; Peyerimhoff, S. D. *Chem. Phys. Lett.* **1972**, *16*, 244. (b) Dunning, T. H., Jr.; Hosteny, R. P.; Shavitt, I. *J. Am. Chem. Soc.* **1973**, *95*, 5667. (c) Hosteny, R. P.; Dunning, T. H., Jr.; Gilman, R. R.; Pipano, A.; Shavitt, I. *J. Chem. Phys.* **1975**, *62*, 4764. (d) Buenker, R. J.; Shih, S.; Peyerimhoff, S. D. *Chem. Phys. Lett.* **1976**, *44*, 385. (e) Luippold, D. A. *Ibid.* **1976**, *43*, 55. (f) Niscimento, M. A. C.; Goddard, W. A., III, *Ibid.* **1979**, *60*, 197; *Chem. Phys.* **1979**, *36*, 147.

(14) Schulten, K.; Ohmine, I.; Karplus, M. *J. Chem. Phys.* **1976**, *64*, 4422. Ohmine, I.; Karplus, M.; Schulten, K. *Ibid.* **1978**, *68*, 2298.

(15) Tavan, P. Schulten, K. *J. Chem. Phys.* **1979**, *70*, 5407. Birge, R. R.; Pierce, B. M. *Ibid.* **1979**, *70*, 165.

(16) Čížek, J.; Paldus, J.; Hubač, I. *Int. J. Quant. Chem.* **1974**, *8*, 951.

0002-7863/83/1505-6211$01.50/0

for this class of compounds. This more recent experimental and theoretical work has vindicated the early predictions.[5-9]

Most of the recent attention has been focused on the problem of the ordering of the lowest excited A_g and B_u states. This is analogous to the problem of the ordering of the L_b and L_a states in cyclic π-electron systems derived from a $(4N + 2)$-electron [$4N$ + 2]annulene perimeter.[18-20] Two factors are of primary importance:[21] (i) first-order CI between degenerate singly excited configurations in the PPP model, which produces "plus" and "minus" states as defined by Pariser,[20] and (ii) CI with multiply excited configurations. Calculations suggest that the former dominates in the cyclic π-electron systems and the latter in the polyenes, and it is natural to ask about the origin of the difference. The two classes of molecules differ in topology (arrangement of primary bonding interaction) and in geometry. Either of these two factors alone or both simultaneously could be responsible and it is therefore of interest to investigate a group of polyenes whose geometry resembles that of the cyclic molecules but whose toplogy remains linear.

We now wish to report the synthesis of a series of conjugated polyenes forced to adopt a hairpin[22] shape by suitable bridging, **1–6**, and a study of their electronic spectra. The geometrical structures of **1–6** are closely related to those of the bridged [10], [14], and [18]annulenes **7–9** which we studied previously:[23] **1–3** are obtained by cutting one of the perimeter bonds, **4–6** by interrupting cyclic conjugation by insertion of a CH_2 group. The geometrical relationship to the acenes, naphthalene, anthracene, and tetracene, is also obvious.

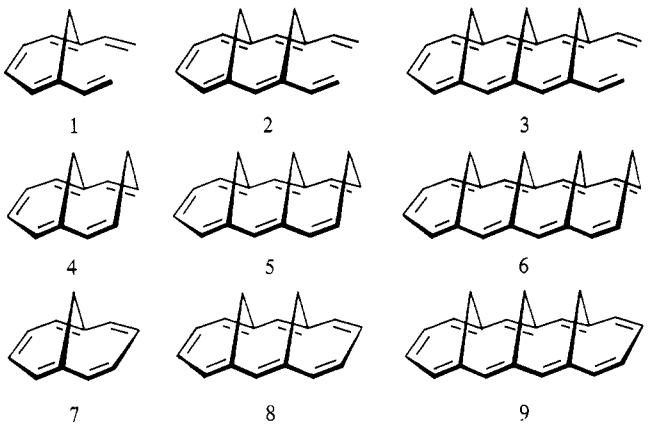

Experimental Section

Materials. General. Melting points are uncorrected. IR spectra were recorded on a Perkin-Elmer 283 spectrometer with films or KBr pellets. UV spectra were obtained on a Model 25 Beckman spectrometer. NMR spectra were determined on a Varian EM-390 spectrometer (90 MHz). Chemical shifts are reported in δ values from tetramethylsilane as internal standard. Low resolution mass spectra were obtained on a Finnigan 3200 mass spectrometer (70 eV) and high resolution mass spectra on a Varian MAT 212 mass spectrometer. For column chromatography Woelm alumina (act. II-III acc. to Brockmann) was used.

1,6-Divinylcyclohepta-1,3,5-triene (1).[24] Triphenylmethylphosphonium bromide (5.36 g, 15 mmol) and sodium bis(trimethylsilyl)amide (2.75 g, 15 mmol) were heated at reflux in 400 mL of absolute THF for $^1/_2$ h under an argon atmosphere. The solution was filtered through an inert gas frit directly into a dropping funnel and then added dropwise over $^1/_2$ h to a solution of 1,6-diformylcyclohepta-1,3,5-triene[25,26] (0.74 g, 5 mmol) in 200 mL of absolute THF. The reaction mixture was stirred for $^1/_2$ h and then filtered through neutral alumina by eluting finally with dichloromethane as solvent. The product obtained was chromatographed on neutral alumina with dichloromethane–pentane. After removal of the solvent distillation of the residue gave 0.5. g (82%) of **1** as a yellow, air sensitive oil: bp 52–53 °C, 0.2 torr; IR (neat) 3100, 3040, 3010, 1617, 1585 cm^{-1}; ^1H NMR (CCl_4) δ 6.05–6.65 (m, 6 H), 5.43 (d, 2 H), 5.04 (d, 2 H), 2.52 (s, 2 H); UV (ϵ) (3-methylpentane) 325 (6200), 242.5 (54000), 236 (44500); mass spectrum M^3 at m/e 144. Anal. Calcd for $C_{11}H_{12}$: C, 91.67; H, 8.33. Found: C, 91.66; H, 8.20.

3,5-Divinylbicyclo[5.4.1]dodeca-2,5,7,9,11-pentaene (2). The procedure outlined above for **1** applied to 3,5-diformylbicyclo[5.4.1]dodeca-2,5,7,9,11-pentaene[26,27] (636 mg, 3 mmol) afforded, after recrystallization of the crude product from hexane, 520 mg (83%) of 2 as yellow crystals: mp 111–112 °C (dec); IR (KBr) 3087, 3026, 1605, 1494 cm^{-1}; ^1H NMR (CCl_4) δ 6.2–6.9 (m, 8 H), 5.47 (d, 2 H), 5.05 (d, 2 H), 3.9 (d, 1 H), 3.75 (d, 1 H), 3.6 (d, 1 H), 0.2 (d, 1 H); UV (ϵ) (3-methylpentane) 367 (5200), 286 (74000), 277.5 (73000); mass spectrum M^3 at m/e 208. Exact mass Calcd for $C_{16}H_{16}$: 208.125194. Found: 208.125648.

5,7-Divinyltricyclo[9.4.1.1^{3,9}]heptadeca-2,4,7,9,11,13,15-heptaene (3). The procedure outlined above for **1** and **2** applied to 5,7-diformyltricyclo[9.4.1.1^{3,9}]heptadeca-2,4,7,9,11,13,15-heptaene[26] (276 mg, 1 mmol) afforded, after recrystallization of the crude product from ethyl acetate–trichloromethane, 204 mg (75%) of **3** as deep yellow needles: 180 °C dec; all physical properties agreed with those reported.[28]

Bicyclo[5.4.1]dodeca-2,5,7,9,11-pentaene (4).[25] To a stirred suspension of trimethylene-1,3-bis(triphenylphosphonium)bromide (7.27 g, 10 mmol) in 150 mL of absolute THF was dropped a solution of *n*-butyllithium (12.1 mL, 1.4 M in hexane) under an argon atmosphere. After stirring for $^1/_2$ h the reaction mixture was filtered through an inert gas frit directly into a dropping funnel and then added dropwise over 2 h to a solution of 1,6-diformylcyclohepta-1,3,5-triene (0.74 g, 5 mmol). The progress of the reaction was followed by thin layer chromatography and the dropping was completed when all the starting material just disappeared. The mixture was stirred for 1 h and then filtered through neutral alumina. The final elution was done with dichloromethane. After removal of the solvent the residue was chromatographed on neutral alumina with pentane–dichloromethane (3:1). The first fraction afforded a yellow oil. Crystallization from pentane yielded 0.35 g (45%) of pure **4** as yellow needles: mp 15 °C; IR (neat) 3044, 3020, 1601, 1557 cm^{-1}; ^1H NMR (CCl_4) δ 6.2–6.9 (m, 6 H), 4.55–5.07 (m, 2 H), 2.6–4.1 (m, 2 H), 3.72 (d, 1 H), 0.21 (d, 1 H); UV (ϵ) (3-methylpentane) 322.5 (3600), 245 (39600); mass spectrum M^3 at m/e 156. Anal. Calcd for $C_{12}H_{12}$: C, 92.26; H, 7.74. Found: C, 92.64; H, 7.73.

Tricyclo[9.4.1.1^{3,9}]heptadeca-2,4,7,9,11,13,15-heptaene (5). The procedure described for the synthesis of **4** applied to 3,5-diformylbicyclo-[5.4.1]dodeca-2,5,7,9,11-pentaene (636 mg, 3 mmol) afforded, after recrystallization of the crude product from hexane, 0.27 g (41%) of **5** as yellow needles: mp 141 °C; IR (KBr) 3040, 2980, 1610, 1510 cm^{-1}; ^1H NMR ($CDCl_3$) δ 6.77–7913 (m, 4 H), 6.57 (s, 2 H), 6.14 (d, 2 H), 4.83–5.18 (m, 2 H), 2.85–4.35 (m, 2 H), 4.25 (d, 1 H), 3.51 (d, 1 H), 3.26 (d, 1 H), 0.66 (d, 1 H); UV (ϵ) (3-methylpentane) 370 (3900), 288 (79500); mass spectrum M^+ at m/e 220. Exact mass Calcd for $C_{17}H_{16}$: 220.125194. Found: 220.125372.

Tetracyclo[9.8.1.1^{3,9}1^{13,18}]docosa-2,4,7,9,11,13,15,17,19-nonaene (6). The procedure described for **4** applied to 5,7-diformyltricyclo-[9.4.1.1^{3,9}]heptadeca-2,4,7,9,11,13,15-heptaene (276 mg, 1 mmol) afforded, after recrystallization of the crude product from hexane–trichloromethane, 80 mg (28%) of **6** as orange plates: 180 °C dec; IR (CsI): 3023, 2940, 1605 cm^{-1}; ^1H NMR ($CDCl_3$) δ 7.05–7.2 (m, 4 H), 6.98 (s, 2 H), 6.32 (s, 2 H), 6.07 (d, 2 H), 4.8–5.17 (m, 2 H), 3.02–4.38 (m, 2 H), 4.42 (d, 1 H), 3.92 (d, 1 H), 3.58 (d, 1 H), 2.83 (d, 1 H), 2.62 (d, 1 H), –0.73 (d, 1 H); UV (ϵ) (3-methylpentane) 400 (5000, sh), 328 (116000), 228 (14000); mass spectrum M^+ at m/e 284. Exact mass Calcd for $C_{22}H_{20}$: 284.1564920. Found: 284.1567138.

Solvents. 3-Methylpentane (3-MP, Phillips Petroleum CO. and EGA-Chemie) and 2-methyltetrahydrofuran (2MTHF) were refluxed with sodium, distilled, and passed over an Al_2O_3–$AgNO_3$ column. Other solvents were spectral grade quality. Because of the limited stability of the polyenes, solutions were always prepared from freshly purified com-

(17) Dick, B.; Hohlneicher, G. *Theoret. Chim. Acta* **1979**, *53*, 221. Herrick, D. R. *J. Chem. Phys.* **1981**, *74*, 1239; Ducasse, I. R.; Miller, T. E.; Soos, Z. G. *Ibid.* **1982**, *76*, 4094.
(18) Platt, J. R. *J. Chem. Phys.* **1949**, *17*, 484.
(19) Moffitt, W. *J. Chem. Phys.* **1954**, *22*, 320, 1820.
(20) Pariser, R. *J. Chem. Phys.* **1956**, *24*, 250.
(21) During the writing of this manuscript we became aware of an independent investigation of this point by J. Koutecký, J. Čížek, J. Paldus, and V. Bonačic-Koutecký (unpublished results). We are grateful to Professor Koutecký for a useful discussion.
(22) This descriptive name has been suggested by Professor Edgar Heilbronner.
(23) Dewey, H. J.; Deger, H.; Frölich, W.; Dick, B.; Klingensmith, K. A.; Hohlneicher, G.; Vogel, E.; Michl, J. *J. Am. Chem. Soc.* **1980**, *102*, 6412.
(24) Vogel, E.; Brinker, U. H.; Nachtkamp, K.; Wassen, J.; Müllen, K. *Angew. Chem.* **1973**, *85*, 760.
(25) Vogel, E.; Feldmann, R.; Düwel, H. *Tetrahedron Lett.* **1970**, 1941.
(26) Vogel, E.; Deger, H. M.; Sombroek, J.; Palm, J.; Wagner, A.; Lex, J. *Angew. Chem.* **1980**, *92*, 43.
(27) Vogel, E.; Sombroek, J.; Wagemann, W. *Angew. Chem.* **1975**, *87*, 591.
(28) Wagemann, W.; Iyoda, M.; Deger, H. M.; Sombroek, J.; Vogel, E. *Angew. Chem.* **1978**, *90*, 988.

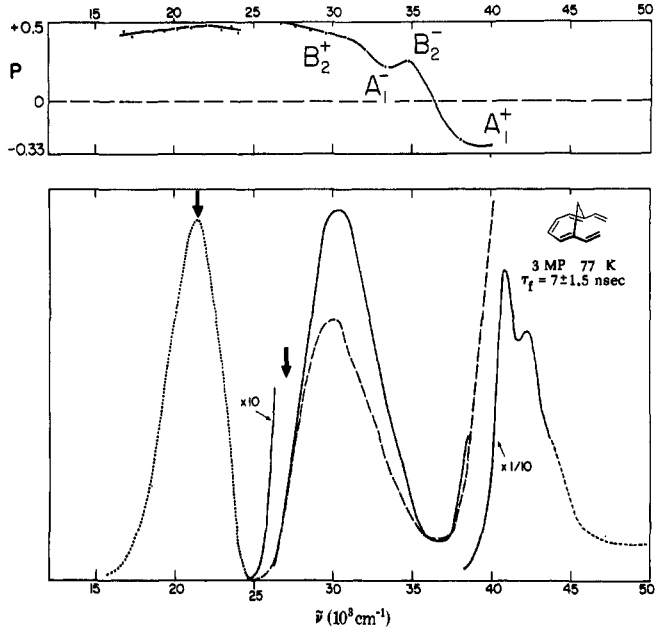

Figure 1. Spectra of the pentaene **1** (3-methylpentane, 77 K). Bottom, absorption (full line), fluorescence (dotted line), and fluorescence excitation (dashed line). Top, fluorescence polarization degree. Wavenumbers of monitoring and excitation are indicated by arrows.

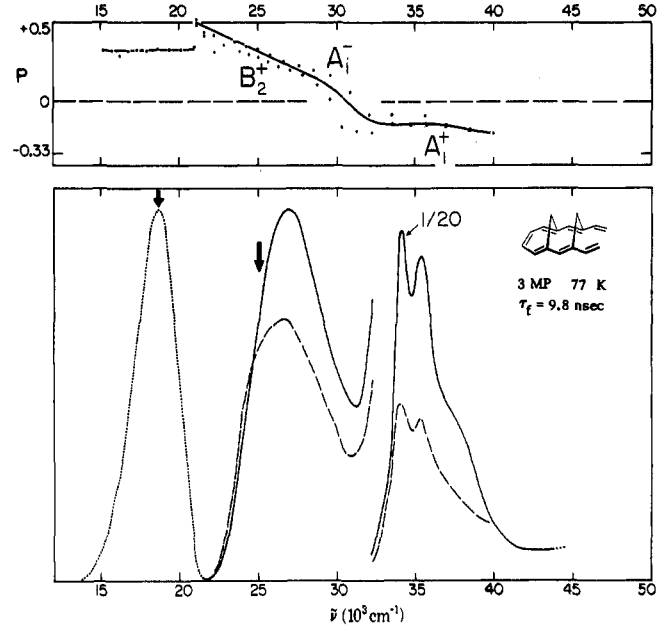

Figure 2. Spectra of the heptaene **2**. See caption to Figure 1.

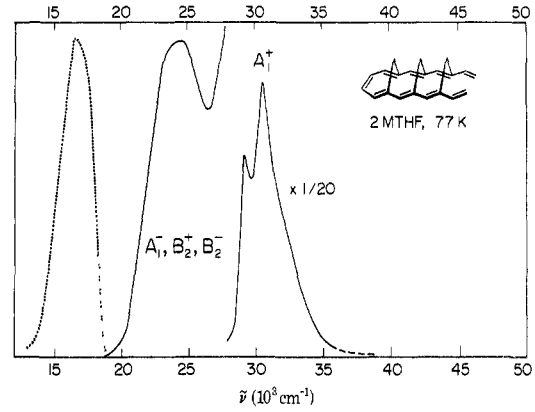

Figure 3. Spectra of the nonaene **3**. See caption to Figure 1.

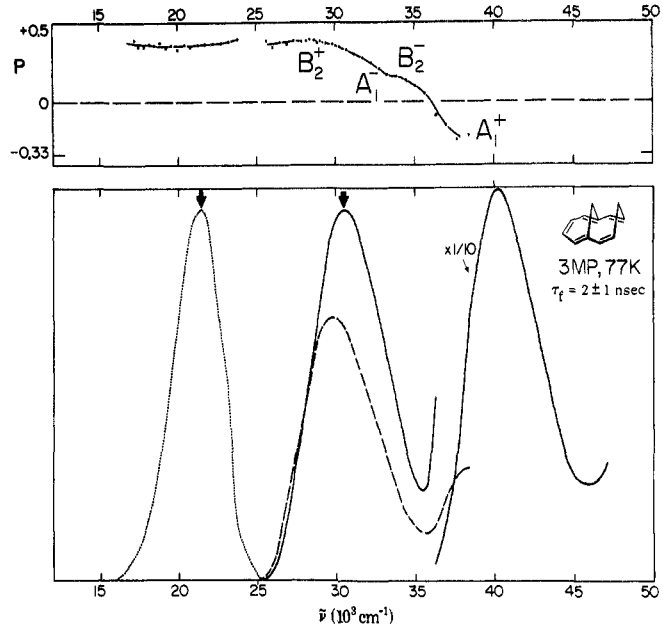

Figure 4. Spectra of the pentaene **4**. See caption to Figure 1.

pounds, kept under argon atmosphere, and used immediately.

Spectroscopy. All of the measurements were performed at Utah and many were performed independently at Cologne as well.

At Utah, absorption and emission spectra in rigid glass were taken in 2-mm Suprasil cells immersed in a quartz Dewar with Suprasil windows, filled with filtered liquid nitrogen. Absorption spectra were measured on a Cary 17 spectrophotometer, polarized fluorescence and fluorescence excitation spectra, as well as fluorescence lifetimes were measured on a home-made instrument described in ref 23. Magnetic circular dichroism was measured at room temperature with a JASCO J-500C spectropolarimeter equipped with a 15-kG electromaget, wavelength calibrated with a holmium oxide filter and scale calibration with the CD of d-camphorsulfonic acid and the MCD of naphthalene as described in ref 29. Linear dichroism of **5** in stretched polyethylene was measured using the techniques of ref 30.

At Cologne, absorption spectra were measured using a Beckmann Acta V spectrophotometer with a commercial low-temperature adaptor. Room temperature measurements were done in 1 cm, low-temperature measurements in 5-mm Suprasil cells. Polarization of emission was measured with a home-made instrument described in ref 31.

Calculations

Since the exact geometries of the hairpin polyenes **1–6** are uncertain, we have restricted our efforts to obtain theoretical guidance in the spectral interpretations to model π-electron calculations of the PPP type. These were performed similarly as in ref 23, assuming planar geometries with 2.4 Å distances between carbon atoms connected by bridges. Double bonds were 1.37 Å and single bonds 1.45 Å long. In the calculations for all-trans polyenes, the bond angles were 120°. The CI was limited to the 100 lowest energy singly and doubly excited configurations for **1** and **4**, 150 for **2** and **5**, and 200 for **3** and **6**. This produced an energy cutoff near 13 eV for **1** and **4** and only about 11 eV for **3** and **6**. Several different choices of two-center electron repulsion integrals were used, with predictable[7] effects on the results. The results reproduced in the Tables were obtained using the Dewar–Ohno–Klopman[32] approximation.

The effect of transannular interaction was simulated by introducing non-nearest-neighbor resonance integrals of equal magnitude between all pairs of atomic orbitals separated by one

(29) Waluk, J. W.; Chivers, T.; Oakley, R. T.; Michl, J. *Inorg. Chem.* **1982**, *21*, 832.
(30) Thulstrup, E. W.; Michl, J. *J. Am. Chem. Soc.*, **1982**, *104*, 5594, and references therein.
(31) Frölich, W., Ph.D. Dissertation, University of Cologne, Germany, 1979.
(32) Dewar, M. J. S.; Hojvat (Sabelli), N. L. *J. Chem. Phys.* **1961**, *34*, 1232. *Proc. R. Soc. London, Ser. A*, **1961**, *264*, 431; Ohno, K. *Theor. Chim. Acta* **1964**, *2*, 219; Klopman, G. *J. Am. Chem. Soc.* **1964**, *86*, 4450.

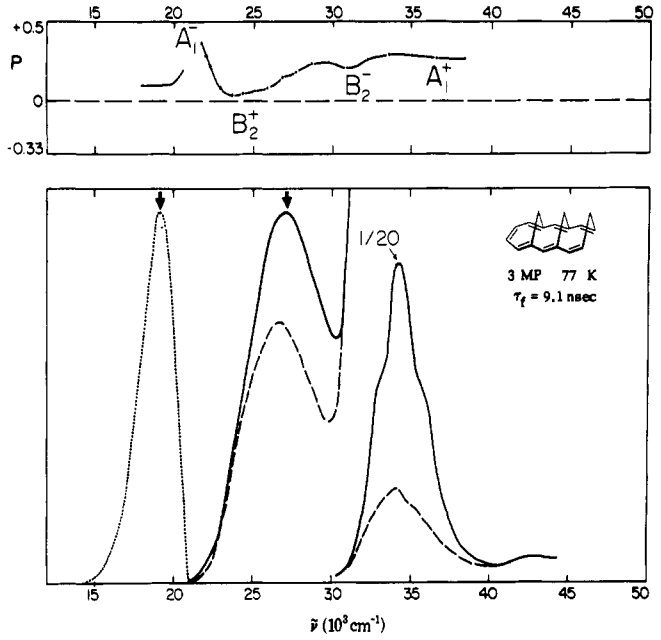

Figure 5. Spectra of the heptaene **5**. See caption to Figure 1.

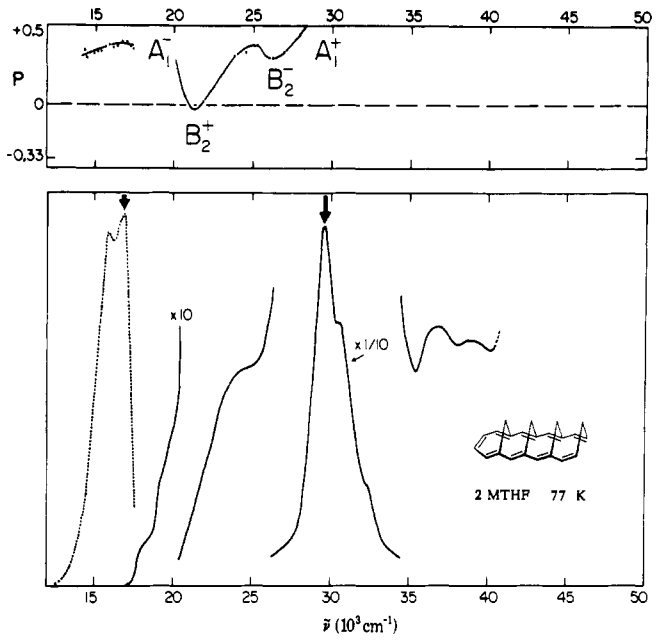

Figure 6. Spectra of the nonaene **6** in 2-methyltetahydrofuran. See caption to Figure 1.

methylene bridge. Their magnitude was varied from zero to $\beta/2$.

Results

Low-temperature absorption and fluorescence spectra of the hairpin polyenes **1–6** are shown in Figures 1–6, respectively. The top part of each figure displays the polarization degree of the fluorescence measured as a function of the excitation energy (monitored at wavenumbers indicated by arrows in the lower part of the figure) and measured as a function of emission energy (excited at wavenumbers similarly indicated). Figures 7 and 8 give the room-temperature absorption (Table I) and MCD spectra of **1–3** and **4–6**, respectively. The MCD signals are an order of magnitude weaker than those observed for the previously studied annulenes with full cyclic conjugation,[23] as is usual for molecules with acyclic chromophores. The MCD spectra are therefore relatively noisy in the regions of strong absorption.

Each absorption spectrum is dominated by one very intense transition which we assign as the long-axis polarization $A_1 \rightarrow A_1$ excitation analogous to the "cis band" of ordinary polyenes containing a single central cis linkage.[33] The reasons for this assignment are described in the Discussion section. The energy of this $A_1 \rightarrow A_1$ excitation decreases regularly as the length of the conjugated chain increases from 40 000 cm^{-1} in **1** and **4** to 30 000 cm^{-1} in **3** and **6**. At the same time, its intensity grows essentially linearly with the length of the molecule (Table I). This transition is relatively weak in MCD. Its B term is weakly positive in the pentaenes **1** and **4** and gradually changes to weakly negative as one proceeds to the nonaenes **3** and **6**. The long-axis polarization of this transition in **5** was verified by the measurement of linear

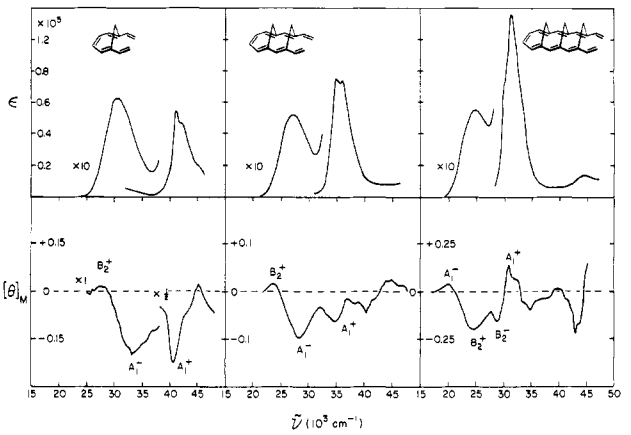

Figure 7. Room temperature MCD (bottom) and absorption (top) spectra of **1**, **2**, and **3** in 3-methylpentane.

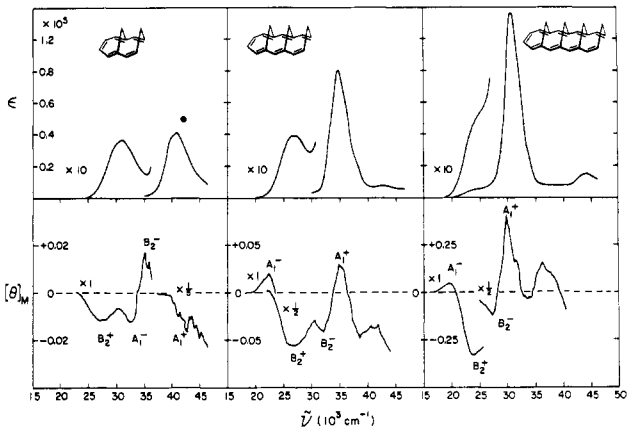

Figure 8. Room temperature MCD (bottom) and absorption (top) spectra of **4**, **5**, and **6** in 3-methylpentane.

Table I. Absorption Spectra in 3-Methylpentane[a]

	$\tilde{\nu}_{max}$, cm^{-1}	ϵ_{max}	f[b]
1	30 800	6 200	0.17
	41 200	54 000	1.02
	42 400	44 500	1.02
2	27 200	5 200	0.13
	35 000	74 000	1.46
	36 000	73 000	1.46
3	24 800	5 500	0.12
	31 300	115 000	1.92
	44 600	14 000	0.34
4	31 000	3 600	0.095
	40 800	39 600	1.01
5	27 000	3 900	0.095
	34 700	79 500	1.42
	43 000	7 000	~0.15
6	25 000	5 000	0.10
	30 500	116 000	1.85
	43 900	14 000	0.34

[a] Room temperature. [b] Oscillator strength computed from the total area of the first absorption band (assigned to three overlapping transitions in the text).

(33) Zechmeister, L. *Chem. Rev.* **1944**, *34*, 267. Eckert, R.; Kuhn, H. *Z. Elektrochem.* **1960**, *64*, 356; see also ref 2b.

dichroism in stretched polyethylene, which yielded a positive dichroic ratio of 2.6 (K_z = 0.56; cf. ref 30).

The absorption spectra show only one additional and much weaker band. Its energy is less sensitive to the chain length, 30 000 cm^{-1} in **1** and **4** and 25 000 cm^{-1} in **3** and **6**. Its intensity is essentially independent of the length of the molecule (Table I). In stretched polyethylene, absorption of **5** in this region exhibits a dichroic ratio of about 1.0, indicating that it is predominantly short-axis polarized, but the relative weakness of the signal due to low solubility of **5** in polyethylene makes a detailed analysis difficult. However, inspection of the polarization curves and of the MCD spectra shows quite clearly that there actually are at least three transitions at energies below that of the "cis band". Their assignments as a weak A_1 transition, a weak B_2, and a stronger B_2 transition are shown in the figures and are based on the following considerations (all observed low-energy states are assumed to be of $\pi\pi^*$ character; the assignment of "plus" and "minus" states will be discussed below).

Pentaenes 1 and 4 (Figures 1, 4, 7, and 8). The fluorescent transition is polarized perpendicular to the "cis band" and is therefore assigned to a B_2 excited state. It has a weak negative B term in the MCD of **1** and a positive B term in **4**. The MCD peak occurs at 27 000–28 000 cm^{-1}, clearly below the absorption peak, indicating that the absorption peak is a composite due to the $A_1 \rightarrow B_2$ transition overlapped by another one. Indeed, the high-energy side has a distinctly lower degree of polarization, showing that the second overlapping transition is of A_1 symmetry. Its presence is quite obvious in the MCD spectrum through a negative peak at 32 000–33 000 cm^{-1} (positive B term). A weak third transition is indicated near 35 000 cm^{-1} by a return of the degree of polarization to higher values for **1**, seen only as an indistinct shoulder in **4**, and we assign it to an excited state of B_2 symmetry. It is not apparent in the MCD of **1**, but is quite clear in the MCD of **4** as a positive peak.

Heptaenes 2 and 5 (Figures 2, 5, 7, and 8). In **2**, the fluorescent transition is again polarized perpendicular to the "cis band" and therefore assigned to a B_2 state, but in **5**, the opposite is true, so that here, the fluorescent state is of A_1 symmetry. These transitions are seen as weak positive peaks in the MCD spectra (negative B terms), located at 23 000–24 000 cm^{-1}, far below the absorption maximum. This once again suggests that the absorption band is a composite. The rapid decrease of the degree of polarization confirms this and provides an A_1 assignment for the second excited state in **2** and a B_2 assignment in **5**. In **5**, it cannot be accounted for by vibronic coupling, since no B_2 transitions of any intensity to speak of appear up to quite high energies, and we assume that the situation is similar in **2**. The order of the A_1 and B_2 states is thus reversed in the two compounds. The second excited states of **2** and **5** are clearly reflected in their MCD spectra as negative peaks at 27 000–28 000 cm^{-1}. A third transition, at about 32 000 cm^{-1}, is present as a negative peak in the MCD of **5**, but cannot be distinguished in the MCD spectrum of **2** where it appears to overlap with the peak of the "cis band", which is also negative. Its existence is also indicated in the polarization curves of **5** by a dip near 31 000 cm^{-1}, which leads us to assign the excited state symmetry as B_2.

Nonaenes 3 and 6 (Figures 3, 6, 7, and 8). The emission intensity for **3** was too weak for a reliable measurement of the polarization degree. In **6**, the fluorescent state is of A_1 symmetry and corresponds to the weak shoulder beginning near 18 000 cm^{-1} in the low-temperature absorption spectrum. This is thus the first case in which the emitting transition is observed directly in absorption rather than only in the MCD and polarization spectra. As one proceeds to higher energies, the polarization degree drops precipitously, showing that the first transition is rapidly followed by a second oppositely polarized one. In MCD spectra of **3** and **6**, the first (A_1) transition appears as a positive peak near 20 000 cm^{-1} and the second (B_2) transition as a negative peak near 24 000 cm^{-1}. A third transition is indicated by a negative peak near 28 000 cm^{-1} in the MCD spectra of **3** and **6** which corresponds to a dip in the degree of polarization observed near 27 000 cm^{-1}. This shows that the excited state is of B_2 symmetry.

Table II. Observed Energies of Excited Singlet States of Polyenes and Bridged [4*N* + 2]Annulenes[a]

	hairpin polyene		all-trans polyene[b]		bridged annulene[c]	
pentaene	A_1^-	33	A_g^-	25	B_{3u}^- (L_b)	25
	B_2^+	27	B_u^+	30	B_{2u}^+ (L_a)	31
	(B_2^-	35)[d]			B_{2u}^+ (B_a)	38
	A_1^+	41			B_{3u}^+ (B_b)	39
heptaene	A_1^-	~25			B_{3u}^- (L_b)	20
	B_2^+	~25	B_u^+	25.6	B_{2u}^+ (L_a)	25
	(B_2^-	32)[d]			B_{2u}^+ (B_a)	32
	A_1^+	35			B_{3u}^+ (B_b)	33
nonaene	A_1^-	18			B_{3u}^- (L_b)	16
	B_2^+	24	B_u^+	23.3	B_{2u}^+ (L_a)	20
	(B_2^-	27)[d]			B_{2u}^+ (B_a)	26
	A_1^+	30			B_{3u}^+ (B_b)	28

[a] Energies in units of 1000 cm^{-1}. State labels are based on C_{2v} symmetry for the hairpin polyenes, C_{2h} symmetry for the all-trans polyenes, and D_{2h} symmetry for the annulenes, for which the Platt notation is also stated. [b] B_u^+ energies[34] and A_g^- energy[11r] were taken from the literature (0-0 bands). The value for octadecanonaene is interpolated between those reported for hexadecaoctaene and for eicosadecaene. [c] Data for methano-bridged annulenes **7–9** from ref 23. [d] This transition is believed not to correspond to the B_{2u}^+ (B_a) transition in the annulenes **7–9**, but to a higher energy transition (see text).

In **3** and **6**, the presence of two additional transitions on the high-energy side of the "cis band" is indicated in the absorption and MCD spectra, but we have no information on their polarization directions.

In summary, the weak low-energy band in **1–6** is composed of transitions to two excited states, one of A_1 and one of B_2 symmetry, and the transition which we have assigned—so far with limited justification—as the $A_1 \rightarrow A_1$ excitation corresponding to the "cis band" is accompanied on its low-energy side by another transition to a state of B_2 symmetry. The composite nature of the first observed absorption band in **1–6** is fully supported by the large Stokes shift and small degree of spectral overlap between the fluorescence and absorption. This is true even for **3**, for which no polarization data are available. The combination of polarized emission and MCD spectroscopy has proved to be particularly fortunate in that the joint evidence for the existence and assignments of weak transitions is much more convincing than either one taken alone.

Table II provides a survey of the experimental results for the hairpin polyenes **1–6** and a comparison with all-trans polyenes and with the bridged annulenes **7–9**. The assignments of approximate "plus" and "minus" symmetry to the excited states given there and in the figures are based on calculations alone as discused below, except that the lower B_2 state and the "cis band" A_1 state clearly must be of "plus" character on account of their intensities.

The table shows that the A_1^- state moves to lower energies faster than the B_2^+ state as the polyene chain grows in length. In the pentaenes, the order is A_1^- above B_2^+, in the heptaenes, the two states are so close in energy that already the bridging of the terminal vinyl groups reverses their order (in **2**, B_2^+ below A_1^-; in **5**, A_1^- below B_2^+), and in the nonaenes, the order is A_1^- below B_2^+ (this has been proven for **6** and only conjectured for **3**). This behavior is qualitatively the same as that of the all-trans polyenes, in which a A_g^- state moves below a B_u^+ state as the length of the polyene chain grows, but a quantitative difference is apparent: in the all-trans series, the A_g^- state certainly lies below B_1^+ already in the tetraene, and possibly even in the triene.[11,12]

Discussion

The juxtaposition of the results for the hairpin polyenes **1–6** and the known results for all-trans polyenes in Table II shows interesting differences which call for an interpretation. First, we shall discuss the qualitative predictions of a simple four-orbital model. The resutls for transition intensities and polarizations permit an assignment of the two observed A_1 states and the lowest B_2 state. The results for energies account for some of the differences between the all-trans and the hairpin polyenes. Second,

Table III. A Section of the CI Matrix for Low-Energy Excited Singlet States of a Symmetrical Alternant Hydrocarbon[a]

	$1 \rightarrow 2$	$0 \rightarrow 3$	$1 \rightarrow 3$	$0 \rightarrow 2$	$1,1 \rightarrow 2,2$
$1 \rightarrow 2$	$\epsilon_2 - \epsilon_1 - (11\|11) + 2(12\|12)$	$2(12\|03) - (01\|01)$	0	0	0
$0 \rightarrow 3$		$\epsilon_3 - \epsilon_0 - (00\|00) + 2(03\|03)$	0	0	0
$1 \rightarrow 3$			$\epsilon_2 - \epsilon_0 - (00\|11) + 2(02\|02)$	$2(02\|02) - (01\|01)$	$\sqrt{2}(01\|12)$
$0 \rightarrow 2$				$\epsilon_2 - \epsilon_0 - (00\|11) + 2(02\|02)$	$-\sqrt{2}(01\|12)$
$1,1 \rightarrow 2,2$					$2[\epsilon_2 - \epsilon_1 - (11\|11) + (12\|12)]$

[a] The matrix is symmetric; only the upper corner is shown. The energy of the ground state has been subtracted along the diagonal.

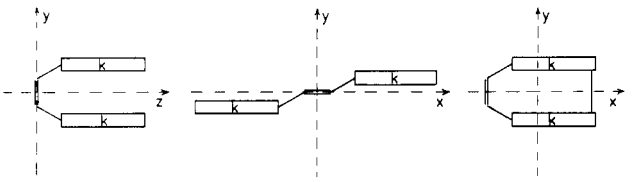

Figure 9. A schematic representation of hairpin (left) and all-trans (center) polyenes, and of bridged [4*N* + 2]annulenes (right).

we shall address finer detail in the spectra and the assignment of the second observed B_2 state using the numerical results of PPP calculations. The obvious shortcomings of the approximation adopted (restricted CI, idealized geometry, no $\sigma\pi^*$ and $\pi\sigma^*$ excitations, etc.) limit the quantitative significance of the results, but in our opinion, do not destroy their usefulness.

Qualitative Analysis. A schematic representation of the hairpin polyenes **4–6** and of the corresponding all-trans polyenes (Figure 9) shows that they can be viewed as composed of a double bond linked to two identical all-trans polyene segments. Each has $2k$ π-electrons, so that the total number of π-electrons is $4k + 2$ and the corresponding annulenes **7–9** obey the Hückel rule. **1–3** may exist in the same spatial arrangement, but one or both of their terminal vinyl groups may also be turned outward. The effects of such a distortion will be discussed later. The idealized planar geometry of the hairpin polyenes possesses the symmetry C_{2v}; the corresponding all-trans polyenes are of symmetry C_{2h}.

The results of all-trans polyenes mentioned in the Introduction suggest that it may be possible to understand the low-energy excited states of the hairpin polyenes in terms of excitations involving only the highest two occupied π molecular orbitals, $2k$ and $2k + 1$, and the lowest two unoccupied MO's, $2k + 2$ and $2k + 3$ (Figure 10). In shorthand notation, we shall refer to these orbitals as *0*, *1*, *2*, and *3*, respectively. The expected low-energy configurations and the resulting states are shown in Figure 11, which also lists their symmetries along with those of the analogous all-trans polyenes and acenes (or annulenes of the type **7–9**). In the PPP approximation, the configurations $1 \rightarrow 3$ and $0 \rightarrow 2$ are degenerate for all alternant π systems because of the alternant pairing symmetry and their interaction produces a "plus" and a "minus" state in the sense of Pariser.[20] The "minus" state further tends to mix strongly with multiply excited configurations, whereas "plus" states are affected much less.[16] The lowest-energy doubly excited configuration, shown in Figure 11, is known to contribute significantly to the A_g^- state of linear polyenes in spite of its relatively high energy.[5-8,13-17]

Configuration degeneracies lead to "minus" and "plus" states in all alternant π-electron systems and in that sense Figure 11 applies in general. However, detailed state odering depends on the relative energies of the four orbitals $2k$ to $2k + 3$ and on electron repulsion terms.

This is best appreciated by inspection of the CI matrix given in Table III for the case of symmetrical molecules for which there is no interaction between either of the configurations $1 \rightarrow 2$ and $0 \rightarrow 3$ and either of the configurations $1 \rightarrow 3$ and $0 \rightarrow 2$. The pairing properties of the MO's were used to simplify the matrix. The section shown is adequate for the present purposes but other doubly excited configurations would have to be added if orbitals

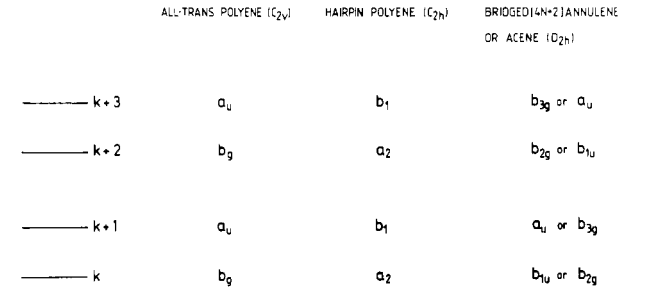

Figure 10. A molecular orbital diagram for polyenes and bridged [4*N* + 2]annulenes (schematic). Transannular interaction under the bridges, as known to occur in **7–9**, is assumed as the source of splitting of the HOMO and LUMO of the [4*N* + 2]annulene. The polyacenes result when the transannular interaction reaches the strength of that of neighbors in the perimeter.

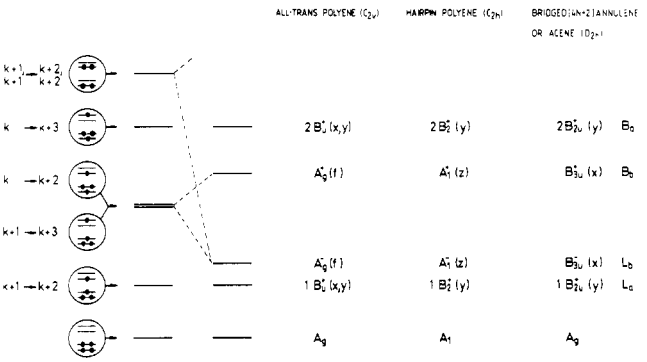

Figure 11. A schematic configuration and singlet state diagram for polyenes and bridged [4*N* + 2]annulenes (acenes are a special case of the latter with strong transannular interaction). The lowest two excited states can occur in either order (schematic).

0 and *1* and orbitals *2* and *3* are nearly degenerate, or exactly degenerate as is the case in the parent (unbridged) annulenes.

A comparison of π-systems which differ in geometry but not in toplogy is relatively simple since the orbital energies ϵ_i in the two systems are nearly identical (they are exactly identical at the Hückel level). For instance, in our PPP calculation, the orbital energies of an all-trans polyene and a hairpin polyene of equal size never differ by more than about 1000 cm^{-1}. Within this approximation, the effects of molecular geometry on transition energy originate primarily in the two-electron terms. The integral (ij/kl) stands for the electrostatic repulsion between the density distribution described by the overlap charge density $e\psi_i\psi_j$ and the density distribution described by $e\psi_k\psi_l$. If $i = j$, $e\psi_i\psi_j$ is the charge density provided by an electron residing in orbital ψ_i and is negative everywhere. If $i \neq j$, $e\psi_i\psi_j$ is negative in those parts of space where ψ_i and ψ_j have the same sign and positive in those parts of space where ψ_i and ψ_j have opposite signs. In the zero differential overlap approximation, the numerical values of the integrals can be readily computed from the knowledge of MO coefficients and electron repulsion integrals between atomic charge densities, but even this is unnecessary if we only wish to obtain a qualitative understanding of trends.

Table IV. Hairpin and All-Trans Polyenes: Difference in the CI Matrices[a]

	$1 \rightarrow 2$	$0 \rightarrow 3$	$1 \rightarrow 3$	$0 \rightarrow 2$	$1,1 \rightarrow 2,2$
$1 \rightarrow 2$	$-\Delta(S_2\|S_2) + 2\Delta(A_3\|A_3)$	$2\Delta(A_2\|A_3) - \Delta(A_1\|A_1)$			
$0 \rightarrow 3$		$-\Delta(S_1\|S_1) + 2\Delta(A_2\|A_2)$			
$1 \rightarrow 3$			$-\Delta(S_1\|S_2) + 2\Delta(S_3\|S_3)$	$2\Delta(S_3\|S_3) - \Delta(A_1\|A_1)$	$\sqrt{2}\Delta(A_1\|A_3)$
$0 \rightarrow 2$				$-\Delta(S_1\|S_2) + 2\Delta(S_3\|S_3)$	$-\sqrt{2}\Delta(A_1\|A_3)$
$1,1 \rightarrow 2,2$					$-2\Delta(S_2\|S_2) + \Delta 2(A_3\|A_3)$

[a] The matrix is symmetric; only the upper corner is shown.

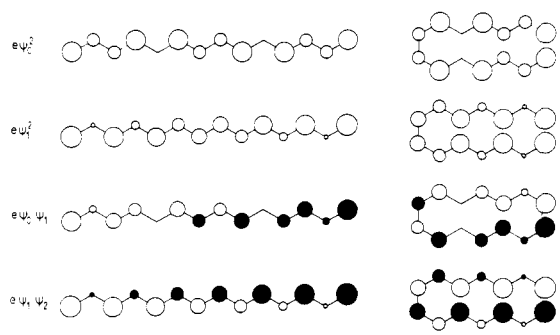

Figure 12. Charge density distributions $e\psi_1^2$, $e\psi_2^2$, $e\psi_1\psi_2$, and $e\psi_2\psi_3$ in the hairpin and all-trans heptaenes. Circled areas are proportional to atomic charges (white: negative, black: positive).

Orbital symmetries listed in Figure 10 show that the charge densities $A_1 = e\psi_0\psi_1$, $A_2 = e\psi_0\psi_3$, and $A_3 = e\psi_1\psi_2$ are antisymmetric relative to the center of the polyene chain (i.e., one terminus carries a positive charge, the other terminus a negative charge), while the other charge densities, $S_1 = e\psi_0^2$, $S_2 = e\psi_1^2$, and $S_3 = e\psi_0\psi_2$, are all symmetric. The difference of the CI matrix for an all-trans polyene and of the CI matrix for a hairpin polyene can then be written symbolically as shown in Table IV where $\Delta(ij/kl) = (ij/kl)_{\text{all-trans}} - (ij/kl)_{\text{hairpin}}$.

In those cases where the symmetries of the charge densities $e\psi_i\psi_j$ and $e\psi_k\psi_l$ are identical, the signs of $\Delta(S|S)$ and $\Delta(A|A)$ are easily derived by inspection of Figure 12. This figure shows the densities obtained from the MO's of the heptaenes but a consideration of the general formula for Hückel MO's of polyenes shows that analogous drawings result for all polyenes.

The repulsion energy due to two charge distributions spread over the same atomic framework is composed of contributions of several kinds. Those due to interactions of partial charges located on the same atom, and those due to partial charges located one bond part, are invariant to changes in molecular geometry since we assume constant bond lengths and angles. The interaction of partial charges separated by three or more bonds will be reduced if like charges are kept apart and/or unlike charges close together. As shown in Figure 12, this is accomplished at the all-trans geometry for the case $(S|S)$ and at the hairpin geometry for the case $(A|A)$. Therefore, $\Delta(S|S) < 0$ and $\Delta(A|A) > 0$.

The signs of $\Delta(S|S)$ and $\Delta(A|A)$ deduced from these qualitative considerations are in full agreement with the results of numerical calculations; the exact values depend on the choice of the two-center two-electron repulsion function. The results for the Ohno parameters are listed in Table V.

With this information in hand, it is easy to visualize most of the entries of Table IV, which symbolizes the difference between the CI matrices of all-trans and hairpin polyenes. Only two distinct entries in the difference matrix have signs which do not follow directly from the known signs of $\Delta(S|S) < 0$ and $\Delta(A|A) > 0$. For one of those, the diagonal element of configurations $1 \rightarrow 3$ or $0 \rightarrow 2$, a prediction is possible when it is recalled that repulsion integrals of the Coulomb type are generally an order of magnitude larger than those of the exchange type, so that $|\Delta(S_1|S_2)| \gg 2|\Delta(S_3|S_3)|$. The other is the interaction element between configurations $1 \rightarrow 2$ and $0 \rightarrow 3$; inspection of Figure 12 suggests strongly that $|\Delta(A_1|A_1)| > |\Delta(A_2|A_3)|$. The other is the interaction element between configurations $1 \rightarrow 2$ and $0 \rightarrow 3$; inspection of Figure 12 suggests strongly that $|\Delta(A_1|A_1)| > |\Delta(A_2|A_3)|$. Both conclusions are confirmed by numerical calculations (Table V).

Table V. Orbital Energy Differences and Electron Repulsion Integrals for Polyenes[a]

	pentaene		heptaene		nonaene	
	all-trans	hairpin	all-trans	hairpin	all-trans	hairpin
$\epsilon_3 - \epsilon_0$	11.078	10.852	9.556	9.302	8.648	8.372
$\epsilon_3 - \epsilon_1$	9.465	9.354	8.410	8.246	7.796	7.588
$\epsilon_2 - \epsilon_1$	7.852	7.856	7.264	7.190	6.944	6.805
$(S_1\|S_1)$	4.59	5.37	3.84	4.72	3.36	4.29
$(S_2\|S_2)$	4.97	5.35	4.27	4.86	3.79	4.39
$(S_1\|S_2)$	4.52	5.23	3.75	4.54	3.24	4.06
$(S_3\|S_3)$	0.57	0.68	0.45	0.57	0.36	0.48
$(A_1\|A_1)$	1.44	0.86	1.36	0.75	1.30	0.68
$(A_2\|A_2)$	0.57	0.51	0.48	0.42	0.41	0.34
$(A_3\|A_3)$	0.67	0.45	0.48	0.29	0.36	0.21
$(A_1\|A_3)$	0.72	0.43	0.59	0.31	0.48	0.22
$(A_2\|A_3)$	0.23	0.08	0.17	0.07	0.13	0.07

[a] PPP model with Dewar-Ohno-Klopman parameters. All values in eV. $S_1 = e\psi_0^2$; $S_2 = e\psi_1^2$; $S_3 = e\psi_0\psi_2$; $A_1 = e\psi_0\psi_1$; $A_2 = e\psi_0\psi_3$; $A_3 = e\psi_1\psi_2$.

Within the framework of the four-orbital model, the geometrical transformation from the hairpin geometry to the all-trans geometry should thus have the following effects on the energies and wave functions of the excited states.

(i) The energies of the transitions $1A^- \rightarrow 1B^+$ and $1A^- \rightarrow 2B^+$ should increase noticeably due to the increase in the diagonal elements. The configurations $0 \rightarrow 3$ and $1 \rightarrow 2$ differ greatly in energy and their interaction is relatively unimportant. It is of interest to note that this qualitative result also accounts for the well-known[35] shift of the all-trans polyene regression line relative to the regression line for more compact hydrocarbons in the plot of the energy of the HOMO $\rightarrow$ LUMO transition in a variety of conjugated hydrocarbons against their Hückel orbital energy difference. Only a fraction of this shift is attributable to the neglect of resonance integral alternation in polyenes in the simple HMO model.

(ii) The energy of the transition $1A^- \rightarrow 1A^+$ should not change much. The increase in the diagonal elements of the $0 \rightarrow 2$ and $1 \rightarrow 3$ configurations should be roughly compensated by the change in their interaction element. For these configurations, even small changes in the interaction element are important, since they are degenerate.

(iii) The energy of the transition $1A^-$ and $2A^-$ should most likely increase somewhat. Both the increased diagonal elements of the configurations $0 \rightarrow 2$ and $1 \rightarrow 3$ and the change in their interaction element toward more negative values will work in this direction. On the other hand, the increase in the matrix element for interaction with the doubly excited configuration $1,1 \rightarrow 2,2$ will tend to lower the energy of this state. While a reliable prediction of the energy change from these qualitative considerations appears impossible, a clear-cut difference in the computational origin of the relatively low energy of the $2A^-$ state can be stated safely. In all-trans polyenes, the low energy of this state is due primarily to the interaction of the $(0 \rightarrow 2)$–$(1 \rightarrow 3)$ combination with the doubly excited configuration $1,1 \rightarrow 2,2$. Indeed, for most choices of parameters and polyene lengths, the interaction element of 0

(34) Sondheimer, F.; Ben-Efraim, D. A.; Wolovsky, R. *J. Am. Chem. Soc.* **1961**, *83*, 1675.
(35) Streitweiser, A., Jr. "Molecular Orbital Theory for Organic Chemists"; Wiley: New York, 1961; Chapter 8. Koutecký, J.; Paldus, J.; Zahradník, R. *J. Chem. Phys.* **1962**, *36*, 3129.

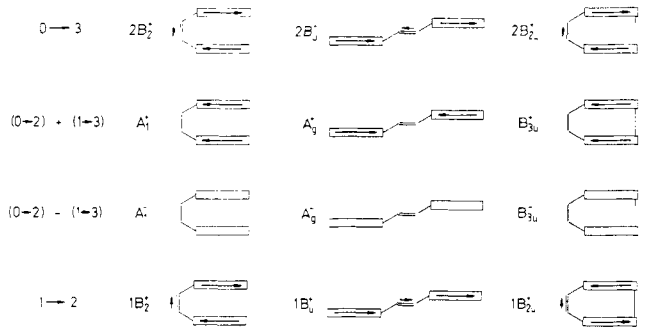

Figure 13. A schematic representation of subunit contributions to transition moments in hairpin and all-trans polyenes and in bridged [4*N* + 2]annulenes (acenes).

$\rightarrow$ *2* with *1* $\rightarrow$ *3* is actually small and negative in all-trans polyenes, so that the A_g^- combination lies above A_g^+, and only the interaction with *1,1* $\rightarrow$ *2,2* brings it down to the vicinity of the $1B_u^+$ state. In hairpin polyenes, the more positive magnitude of the interaction element places A_1^- below A_1^+ to start with, and the mixing with *1,1* $\rightarrow$ *2,2* is now weaker.

The decrease in the importance of mixing with the doubly excited configuration upon going from the all-trans geometry to the hairpin geometry is in accordance with rule 2 of ref 7, which stated that the energy-lowering effects of the introduction of multiply excited states into the CI procedure should be reduced as the molecular geometry is made more compact.

It follows from (i) and (ii) that the energy gap between the $1B^+$ state and the $1A^+$ state should be smaller in all-trans than in hairpin polyenmes. This will be difficult to verify since the location of the $1A_g^+$ state is mostly unknown in the former. Of more immediate interest is a consequence of (i) and (iii) which suggests that one will have to go to a longer polyene in the hairpin than in the all-trans series before the $2A^-$ state moves below the $1B^+$ state. This fits the experimental observations made here for the lowest excited states of A_1 and B_2 symmetry in the hairpin polyenes and agree with their assignment to the theoretically expected $2A_1^-$ and $1B_2^+$ states.

The difference in the composition of the $2A^-$ wave functions in the two series of polyenes outlined in point (iii) is of theoretical interest. After all, the fundamental physical reason why the A^- state is so low in energy (first or second excited state) is that it is of covalent nature; i.e., the VB structures which describe it do not involve the energetically costly separation of charge. An MO procedure with no CI whatever cannot describe this situation since it is not sufficiently flexible to correlate the electons properly. This is accomplished when CI is introduced, and depending on molecular topology and geometry, the bulk of the improvement can be due to interactions among singly excited configurations which are actually doubly excited relative to each other (hairpin polyenes, aromatics) or to interactions with multiply excited configurations (all-trans polyenes). We believe that is is undesirable to refer only to the latter as "correlation effects" (this common usage probably reflects the fact that correlation effects in the *ground state* are primarily described by inclusion of configurations which are multiply excited relative to the ground configuration).

As indicated above, the qualitative conclusions concerning the energies of the A_1^+, $1B_2^+$ and $2B_2^+$ transitions in hairpin polyenes, along with the expectation that A_1^- will lie below A_1^+, probably in the general vicinity of $1B_2^+$, already suggest an assignment of the experimentally observed bands. Before proceeding with such an assignment, we shall also consider the consequences of the four-orbital model for transition moments. For this purpose, it is useful to decompose the molecular electric dipole transition moment into contributions due to the individual parts of the molecule. The results obtained by consideration of the dipole moments of the appropriate overlap densities are shown in Figure 13. In the case of linear polyenes, the partial moments for transitions $1B_u^+$ and $2B_u^+$ are in phase and can be expected to produce a large total moment, increasing with increasing chain length, while the moments for transitions to A_g^+ and A_g^- states vanish. This agrees with the known spectral data for all-trans polyenes, in which the first fully allowed transition ($1B_1^+$) not only shifts to lower energies but also intensifies dramatically as the number of double bonds increases.[34,36]

The situation is quite different for the hairpin polyenes. Only weak intensity is expected for the two B_2^+ transitions, which correspond to the intense B_u^+ transitions of the all-trans polyenes, since the contributions of the terminal sections cancel each other and only the short-axis polarized partial moment produced in the central double bond remains. If the $1B_2^+$ excitation again were to be the first fully allowed transition, as expected from the above analysis, the spectra ought to begin with a relatively weak short-axis polarized band whose intensity does not increase with the increasing size of the polyene (if anything, it should decrease as the participation of the central double bond in the frontier orbitals decreases in importance). This is just the behavior found for the first observed B_2 transition. Since it also appears at similar albeit somewhat lower energies than the B_u^+ transition of linear polyenes of equal size insofar as the latter are known, its assignment as due primarily to the *1* $\rightarrow$ *2* excitation is quite clear. The second relatively weak B_2^+ transition of the hairpin polyenes, due primarily to the *0* $\rightarrow$ *3* excitation, should occur at considerably higher energies. It is not clear from the present qualitative analysis whether it corresponds to the third observed excited state, which has the correct symmetry, or whether it lies at even higher energies. Since the orbital energy difference $\epsilon_3 - \epsilon_0$ is large, particularly in the smaller polyenes, the latter possibility is quite real. The third observed state would then have to originate in excitations involving orbitals other than the four frontier MO's considered presently.

The most intense transition in the hairpin polyenes should correspond to the "cis band" and lead to an excited state of A_1^+ symmetry, (*0* $\rightarrow$ *2*) + (*1* $\rightarrow$ *3*). In this case, the long-axis polarized contributions of the two terminal chains to the transition moment add constructively. The intensity should grow rapidly with the increasing size of the polyene. Thus, there is no doubt as to the assignment of this transition to the most intense observed band, and we have used this as the basis for absolute polarizations in analyzing the experimental results. The results obtained for the absolute polarizations in **5** in stretched polyethylene serve as an additional confirmation. The spectral similarity of the "cis band" to the analogous B_b transition in bridged [4*N* + 2]annulenes[23] is striking and provides further support for the assignment.

The least intense of the four transitions should be that into the A_1^- state, corresponding roughly to (*0* $\rightarrow$ *2*) − (*1* $\rightarrow$ *3*). Unlike the transition into the A_g^- state in all-trans polyenes, it is not forbidden by symmetry. However, both A_1^- and A_g^- are minus states, for which all contributions to transition moments vanish in the case of perfect alternant pairing symmetry. Any actually observed intensity of the A_1^- transition in hairpin polyenes thus represent a measure of the deviation of the actual molecule from the idealized alternant model of the PPP theory. Since only one very weak A_1 transition has been observed experimentally, its assignment to the expected A_1^- state poses no problem.

In summary, then, the qualitative analysis provides assignments of the observed states to one-electron excitations, or their simple mixtures, in the way shown in Table II, except that it is not certain whether the expected $2B_2^+$ transition [*0* $\rightarrow$ *3*] corresponds to the third observed transition or to some higher transition. Of the predictions for the energies of the A_1^+, $1B_2^+$, and $2B_2^+$ transitions in the hairpin polyenes relative to the all-trans polyenes, only that for the $1B_2^+$ can be checked due to the lack of experimental data for the latter. Even here the comparison is made uncertain by the presence of the bridging methylene groups in the hairpin polyenes. The expected increase in the energy of the $1A^- \rightarrow 1B^+$ transition upon going from the hairpin to the all-trans polyenes (point (i) above) is observed for the pentaene. However, there is little change for the heptaene and the nonaene, at least when the position of the lowest of the series of vibronic peaks observed

(36) Suzuki, H. "Electronic Absorption Spectra and Geometry of Organic Molecules"; Academic: New York, 1967.

Table VI. Calculated Energies of Excited Singlet States of Polyenes[a]

pentaene		heptaene		nonaene	
hairpin	all-trans	hairpin	all-trans	hairpin	all-trans
B_2^+ 25.3 (0.062)	**B_u^+ 31.9 (1.91)**	**B_2^+ 21.4 (0.026)**	**B_u^+ 28.3 (2.75)**	**B_2^+ 19.9 (0.017)**	**B_u^+ 25.6 (3.50)**
A_1^- 30.1	**A_g^- 33.1**	**A_1^- 27.8**	**A_g^- 31.9**	**A_1^- 27.1**	**A_g^- 31.4**
B_2^- 37.5	B_u^- 39.4	B_2^- 33.5	B_u^- 37.3	B_2^- 32.3	B_u^- 34.6
A_1^- 42.6	**A_g^+ 45.5**	A_1^- 37.9	**A_g^+ 42.6**	A_1^- 35.8	**A_g^+ 34.9**
A_1^- 45.2	A_g^- 46.2	**B_2^+ 40.3 (0.026)**	A_g^- 45.8	**B_2^+ 36.1 (0.038)**	A_g^- 40.1
B_2^+ 47.6 (0.074)	A_g^- 49.9	A_1^- 40.5	A_g^- 48.0	A_1^- 37.5	**B_u^+ 42.5 (0.50)**
A_1^+ 48.5 (1.74)	B_u^- 51.3	**A_1^+ 41.5 (2.48)**	**B_u^+ 49.0 (0.41)**	**A_1^+ 37.7 (3.26)**	A_g^- 43.8
B_2^- 49.1	**B_u^+ 54.8 (0.33)**	B_2^+ 43.9 (0.33)	B_u^- 49.6	B_2^+ 38.6 (0.30)	B_u^- 44.9
A_1^- 49.8	B_u^+ 55.2 (0.026)	A_1^- 44.1	B_u^+ 51.0 (0.046)	A_1^- 41.2	B_u^+ 45.3 (0.079)
B_2^+ 52.9 (0.32)		B_2^- 46.5		B_1^- 43.2	

[a] In units of 10^3 cm^{-1}. The numbers in parentheses are the oscillator strength f (they vanish for all transitions to "minus" states). The calculations used singly and doubly excited configurations and the Dewar–Ohno–Klopman parameters for electron repulsion integrals.

for this transition in the all-trans polyenes is taken for the vertical transition, as has been done in Table II. As the all-trans polyenes increase in length, the peak of the Franck–Condon envelope of this transition gradually shifts away from the 0–0 transition. Even considering this, the above prediction (i) does not seem to hold too well, and we believe that this is due to the presence of transannular interaction introduced by the presence of the bridging methylene groups, as outlined below.

It is also of interest to compare the spectral properties of the hairpin polyenes to those of the bridged annulenes **7–9**, using the correspondence indicated in Table II. As shown earlier,[23] the orbital degeneracy expected in a regular polygon is removed in **7–9**, primarily by transannular interaction, which yields a frontier orbital ordering similar to that in the acenes.[37] The intensities of the transitions in **7–9** are quite similar to those in **1–6**: the long-axis polarized B_b transition, analogous to $1A_1^+$, is by far the most intense; the long-axis polarized L_b transition, analogous to $1A_1^-$, is very weak. The two short-axis polarized transitions, L_a and B_a, analogous to $1B_2^+$ and $2B_2^+$, respectively, are substantially stronger than L_b but not nearly as strong as B_b. On the other hand, the state energies are quite different except that the cis band of the hairpin polyenes is quite close to the B_b band of the bridged annulenes. A qualitative comparison of the energies is difficult since the molecular topology, and therefore also orbital energies, are quite different in the two classes of compounds.

Having mentioned the presence of transannular interaction in **7–9**, which has been proven beyond doubt,[23] it is interesting to consider its effect on the spectra of **1–6**. The orbital overlap at the points of interaction is disrotatory in all positions in **4–6** and in all except possibly one in **1–3**. The form of the frontier MO's is such that such interaction will stabilize ψ_1 and destabilize ψ_2, without perturbing the alternant pairing symmetry. The orbitals ψ_0 and ψ_3 are set up less favorably for interaction below the bridged atoms. Still, destabilization of ψ_0 and a stabilization of ψ_3 is expected. In the simple model, transannular interaction should increase the energy of $1B_2^+$ transition, thus opposing prediction (i) and accounting for the similarity of the $1A^- \rightarrow 1B^+$ excitation energies in the hairpin and in the linear polyenes (Table II). It should also decrease the energy of the $1A_1^- \rightarrow 2B_2^+$ transition and have little effect on the energies of $1A_1^-$ and $1A_1^+$. This is quite different from that obtained for the bridged annulenes **7–9**, where transannular interaction causes a particularly strong increase in the energy of the L_b transition, which corresponds to the $1A_1^-$ transition of the hairpin polyenes, and has less effect on the L_a transition, which corresponds to $1B_2^+$. The difference is understandable upon inspection of the MO's of the hairpin polyenes and those of the annulenes: transannular interaction will have almost no effect on orbitals ψ_1 and ψ_2 in the annulenes, it will stabilize ψ_0 and destabilize ψ_3. When a hairpin polyene is compared with an acene, it is noted that ψ_0 and ψ_1 have reversed their order, and so have ψ_2 and ψ_3 (in a sense, then, the polyene $1B^+$ state really corresponds to the acene B_a state rather than the acene L_a state!).

Comparison with π-Electron Calculations. The results of our calculations using a relatively small number of singly and doubly excited configurations are shown in Table VI. We note first that the results for the four excited states considered in the qualitative analysis (boldface in Table VI) confirm the qualitative conclusions concerning relative state energies and transition moments. The A_1^- state of the hairpin polyenes is calculated to lie somewhat below the A_g^- state of the corresponding all-trans polyenes but with the limited CI used this may not be a meaningful result.

The lowering of the A_1^- state of hairpin polyenes by admixture of doubly excited configurations is much less pronounced than is the case for all-trans polyenes. At the level of calculation used, doubly excited configurations have a weight of about 25% in the A_1^- state of the hairpin polyenes and about 35% in the A_g^- state of the all-trans polyenes. This is in good agreement with our qualitative picture and with rule 2 of ref 7. The first transitions into "minus" excited states in the hairpin polyenes which are shifted considerably by the introduction of doubly excited configurations are $1B_2^-$ (about 50% doubly excited configurations) and $2A_1^-$.

The effect of transannular interaction was mimicked by including resonance integrals joining the atoms connected by the bridges. Since the exact geometries of **1–6** are unknown, all of these were set equal and their value was varied from 0 to the unrealistically high values of 0.5β. In partial agreement with the qualitative analysis, the energies of the $1A_1^-$ and $1A_1^+$ transitions are affected very little, that of the $2B_2^+$ transition increases somewhat, and that of the $1B_2^+$ transition is strongly shifted to higher energies. In all three polyenes the calculations predict a crossing of the lowest two excited states, $1B_2^+$ and $1A_1^-$, in the region of 0.1β–0.3β for the strength of the transannular interaction.

Before comparing the experimental and calculated spectra, one additional problem must be mentioned for **1–3**. In these compounds one or both terminal vinyl groups can be turned to the outside. The great similarity of the spectra of **1–3** on the one hand and **4–6** on the other hand is no argument against the existence of such conformations, since our calculations suggest only very small differences between the transition energies of the two series of compounds. The only significant difference is that the $1B_2^+$ transition should be intensified in the singly or doubly "turned out" geometries. It is possible that the slightly higher intensity of this transition in **1**, and to a smaller degree also **2** and **3**, relative to **4–6**, is due to the turned-out geometry in some fraction of the molecules.

The agreement of the calculated (Table VI) and experimental (Table II) energies is reasonable but only semiquantitative. The calculated B_2^+ energy is too low and decreases too rapidly with chain length. The calculated A_1^- energy is about right for the pentaene but decreases too slowly with chain length, undoubtedly because the extent of CI used becomes progressively less and less adequate. The observed near degeneracy of B_2^+ and A_1^- is obtained when weak transannular interaction ($\sim 0.2\beta$) is introduced into the calculation, but we hesitate to take this in itself as evidence for its presence since the exaggerated B_2^+–A_1^- split calculated without transannular interaction may be due to other deficiencies

(37) The similarity of the orbital ordering in 1,6-methano[10]annulene **7** and in naphthalene has been recently confirmed by a detailed examination of substituent effects in MCD spectra: Klingensmith, K. A.; Puttmann, W.; Vogel, E.; Michl, J. *J. Am. Chem. Soc.* **1983**, *105*, 3357.

in the method. We believe that the comparison of the relative position of the $1B^+$ transition in the hairpin and the all-trans polyenes, already discussed above, represents more convincing evidence in favor of the presence of transannular interactions in the former.

The energy calculated for the A_1^+ transition is somewhat too high but its shift with the increasing chain length is reproduced well. The calculation suggests that the observed second B_2 transition is not to be assigned as B_2^+ but as B_2^-, which cannot be described within the framework of the four-electron model, and this is the assignment indicated in the Figures 1-8. The change of the order of the $1A_1^-$ and $1B_2^+$ states in the heptaenes (**2**: A_1^- above B_2^+; **5**: A_1^- below B_2^+) may be due to stronger transannular interaction in **5**, which should increase the energy of the $1B_2^+$ state.

Conclusions

It has been possible to locate and assign the A_1^-, B_2^+, and A_1^+ excited states of hairpin polyenes, analogous to the A_g^-, B_u^+, and A_g^+ excited states of all-trans polyenes. In addition, an additional low-energy excited state of B_2 symmetry, presumably B_2^-, has been detected, whose analogue has apparently not yet been observed in the all-trans series. The energies of the transitions in hairpin polyenes differ in a characteristic way from those in all-trans polyenes and this variation, as well as trends in transition intensities, can be understood in terms of simple qualitative considerations.

In both series, the lowest A^- and B^+ states are nearly degenerate. In terms of the MO-CI description, the relatively low energy of the covalent A^- state is well-known to be caused by interactions with multiply excited configurations in the all-trans case. We now find that in the hairpin case it is due largely to interactions within the singly excited part of the CI space, although the interaction with multiply excited configurations also contributes as in all alternant π systems. We provide a simple qualitative explanation for the difference and point out the relation of hairpin polyenes to bridged $[4N + 2]$annulenes and acenes. The qualitative arguments used for the analysis of the dependence of transition energies on molecular geometry (as opposed to topology) have general applicability. For instance, they provide a simple explanation of the lower energy of the B^+ transition in *s-cis*-butadiene relative to *s-trans*-butadiene[38] (the difference is predicted to be smaller in the triplet manifold).

Numerical calculations in the π-electron approximation are in semiquantitative agreement with the experimental results. These calculations, and particularly the comparison of the hairpin with the all-trans polyenes, suggest that weak transannular interactions are present between the bridged carbon atoms in the hairpin polyenes **1-6**.

Acknowledgment. This work was supported by a NATO Research Grant. The authors at Utah acknowledge support from the U.S. National Science Foundation (CHE 81-21122) and the U.S. Public Health Service (GM 21153). J.M. is grateful to the Alexander-von-Humboldt-Stiftung for a Senior U.S. Scientist Research Award and to Professors J. Koutecký (Free University, Berlin) and A. Weller (Max-Planck-Institut für Biophysikalische Chemie, Göttingen) for warm hospitality at their respective institutions during the preparation of this manuscript. The authors at Cologne acknowledge support from the Deutsche Forschungsgemeinschaft, Fonds der Chemischen Industrie, and the Minister Für Wissenschaft and Forschung des Landes Nordsheim-Westfalen. Computer time was provided by Regionales Rechenzentrum der Universität zu Köln.

Registry No. 1, 50785-96-1; **2**, 86846-94-8; **3**, 68539-85-5; **4**, 4692-14-2; **5**, 86846-95-9; **6**, 86846-96-0; 1,6-diformylcyclohepta-1,3,5-triene, 28172-94-3; 3,5-diformylbicyclo[5.4.1]dodeca-2,5,7,9,11-pentaene, 55759-42-7; 5,7-diformyltricyclo[9.4.1.$1^{3,9}$]heptadeca-2,4,7,9,11,13,15-heptaene, 60237-65-2; triphenylmethylphosphonium bromide, 1779-49-3; sodium bis(trimethylsilyl)amide, 1070-89-9; trimethylene-1,3-bis(triphenylphosphonium)bromide, 7333-67-7.

(38) Squillacote, M. E.; Sheridan, R. S.; Chapman, O. L.; Anet, F. A. L. *J. Am. Chem. Soc.* **1979**, *101*, 3657.

Evaluation and Perturbation of Micelle-Solute Interactions[1]

Daniel W. Armstrong* and Gail Y. Stine

Contribution from the Department of Chemistry, Texas Tech University, Lubbock, Texas 79409. *Received February 28, 1983*

Abstract: The interaction of seven compounds (i.e., naphthol green B, bromophenol blue, alizarin red S, 2-naphthol-6-sulfonic acid, ammonium thiocyanate, sodium 2-naphthalenesulfonate, and sodium nitroferricyanide) with sodium dodecyl sulfate (SDS) micelles was studied using LC and TLC. All seven compounds showed unusual chromatographic behavior in that their retention increased when the concentration of micelles in the mobile phase increased. Sometimes a compound's retention behavior was independent of the concentration of micelles in the mobile phase. Based on their chromatographic behavior, all solute-micelle interactions can be classified as *binding*, *nonbinding*, or *antibinding*. Relatively small changes in the micellar environment or the micelle itself can result in pronounced alteration of micelle-solute interactions.

Introduction

The partitioning or binding of compounds to micelles is an important phenomena in many areas of study including membrane mimetic chemistry,[2] catalysis,[3-8] enzyme modeling,[9] chromatography,[10-14] tertiary oil recovery,[15] spectroscopic analysis,[16-18] emulsion polymerization,[19] and so on. There are a variety of

(1) Support of this work by the National Science Foundation (CHE-8119055) is gratefully acknowledged. We also thank Drs. C. A. Bunton and L. S. Romsted for helpful discussion of this work.

(2) Fendler, J. H. "Membrane Mimetic Chemistry"; Wiley: New York, 1982.
(3) Menger, F. M.; Portnoy, C. A. *J. Am. Chem. Soc.* **1967**, *89*, 4698.
(4) Menger, F. M.; Portnoy, C. A. *J. Am. Chem. Soc.* **1968**, *90*, 1875.
(5) Cordes, E. H., Ed. "Reaction Kinetics in Micelles"; Plenum Press: New York, 1973.
(6) Bunton, C. A. *Pure Appl. Chem.* **1977**, *49*, 969.
(7) Fendler, J. H.; Fendler, E. J. "Catalysis in Micellar and Macromolecular systems"; Academic Press: New York, 1975.
(8) Bunton, C. A.; Romsted, L. S.; Savelli, G. *J. Am. Chem. Soc.* **1983**, *105*, 1253.
(9) Fendler, J. H. *Acc. Chem. Res.* **1976**, *9*, 153.
(10) Armstrong, D. W.; Terrill, R. O. *Anal. Chem.* **1979**, *51*, 2160.
(11) Armstrong, D. W.; Henry, S. J. *J. Liq. Chromatogr.* **1980**, *3*, 657.

0002-7863/83/1505-6220$01.50/0